

Supporting information

3D Micropatterned Surface Inspired by *Salvinia molesta* via Direct Laser Lithography.

Omar Tricinci^{,†}, Tercio Terencio^{†,#}, Barbara Mazzolai[†], Nicola M. Pugno^{‡,§,||},
Francesco Greco^{*,†}, Virgilio Mattoli^{*,†}*

[†] Center for Micro-BioRobotics, Istituto Italiano di Tecnologia, Viale Rinaldo Piaggio 34, 56025 Pontedera, Italy

[#] Department of Neuroscience and Brain Technologies, Istituto Italiano di Tecnologia, Via Morego 30, 16163 Genoa, Italy

[‡] Laboratory of Bio-inspired & Graphene Nanomechanics, Department of Civil, Environmental and Mechanical Engineering, University of Trento, via Mesiano 77, 38123 Trento, Italy

[§] Center for Materials and Microsystems, Fondazione Bruno Kessler, via Sommarive 18, 38123 Povo, Italy

^{||} School of Engineering & Materials Science, Queen Mary University of London, Mile End Road, London E1 4NS, UK

Fabrication of Salvinia-Inspired Structures. The design of the salvinia-like structures (Figure 1e) has been programmed with Matlab® (The Mathworks, Inc.). Arrays of regularly arranged artificial hairs were realized in negative tone IP-DiLL photoresist (Nanoscribe GmbH) on a glass substrate, using a direct laser lithography setup, Photonic Professional system (Nanoscribe GmbH). At first the glass substrate has been rinsed with acetone, Isopropyl alcohol (IPA) and deionized water. A thin layer of few nanometers of Indium tin oxide (ITO) has been deposited on the substrate with a DC Magnetron sputtering system, at a power of 80W for 3 min. The ITO layer makes possible the detection of the interface between the substrate and the photoresist. It also ensures a good adhesion of the structures on the glass surface. Finally a drop of IP-DiLL photoresist has been cast on the substrate. The structures were fabricated by exposing the photoresist to a laser beam with a center wavelength of 780 nm, using a writing speed of $100 \mu\text{m s}^{-1}$ with a power of 4.6 mW (Calman laser source). The sample was then developed for 20 min in SU-8 Developer (MicroChem Corp) and rinsed with IPA and deionized water.

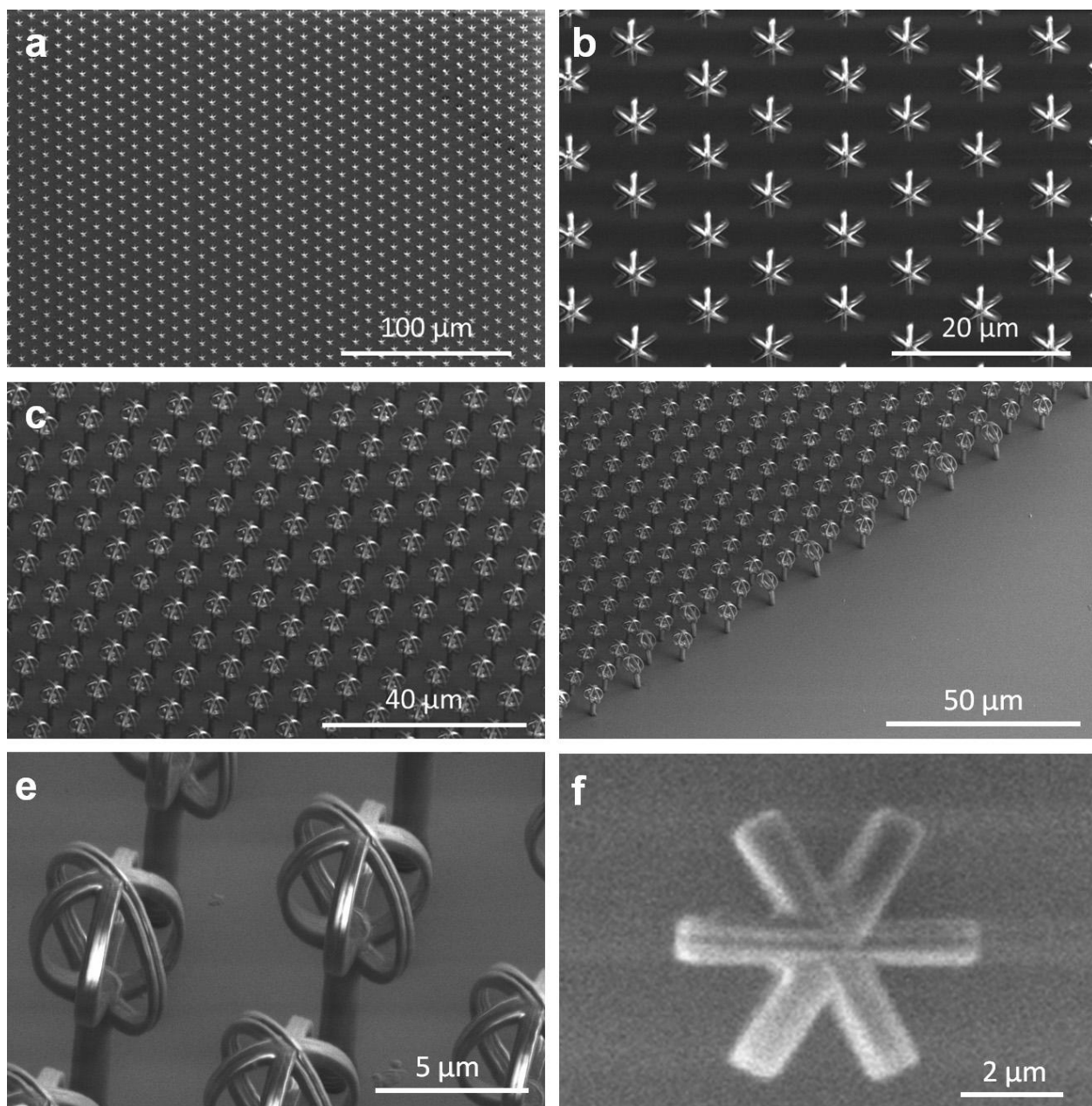


Figure S1. Additional SEM images of the sample presented in main text (square array of hairs with a head-to-head distance of 3 μm; hair parameter: $N = 3$; $r = 3$ μm; $\delta = 1$ μm; $h = 7$ μm; $w = 1.5$ μm) at different magnifications and view angles.

Air trapping test details. In order to evaluate the air trapping capability and visualize the solid-liquid, solid-air and liquid-air interfaces, a confocal microscope (C2 Confocal Microscope System, Nikon) was used. The water used to submerge the sample was marked with a fluorescent probe, Tetramethylrhodamine-5-(and-6)-isothiocyanate (5(6)-TRITC) (Life Technologies), with a concentration of 0.01 mg mL^{-1} in water. The sample surface were observed at the confocal microscope by exciting at two different light wavelengths: 401 nm (excitation wavelength of IP-DiLL photoresist self-fluorescence) and 561 nm (excitation wavelength of TRITC).

All the analysis has been carried out by encapsulating the sample as in the following: a ring of silicone elastomer poly(dimethyl siloxane) (PDMS, Sylgard 184, Dow Corning Corp), with an internal diameter of 8 mm and a thickness of 200 μm , has been placed around the array of hairs on the glass, in order to confine the solution around the array and mainly to avoid optical aberrations due to the spherical shape of the droplet. The ring has been prepared by spin coating PDMS on a glass and then cutting it with a laser cutting system (Versalaser, Universal Laser Systems). After the deposition of the TRITC solution droplet with a volume of about 10 μL , a glass slide was put over the ring, sealing the sample.

Air trapping tests were carried out on different types of samples:

- Square arrays of about 180 μm per side (22x20 hairs) have been preliminary used to study the air trapping phenomenon, checking the presence of the air inside the crown-like heads and, in case, between stalks, by using different geometrical parameters. Only results on best samples (hair parameter: $N = 3$; $r = 3 \text{ }\mu\text{m}$; $\delta = 1 \text{ }\mu\text{m}$; $h = 7 \text{ }\mu\text{m}$; $w = 1.5 \text{ }\mu\text{m}$; head-to-head distance 3 μm), have been shown in the main text. Additional design and test results can be found in the following section.

- Hexagonal arrays with 6 hairs per side in hexagonal arrangement (hair parameter: $N = 3$; $r = 3 \text{ }\mu\text{m}$; $\delta = 1 \text{ }\mu\text{m}$; $h = 7 \text{ }\mu\text{m}$; $w = 1.5 \text{ }\mu\text{m}$) have been used for evaluating the capability of the arrangement of the structures in preventing the entrance of the water between the stalks, by modulating the head-to-head distance (varied from 0 to 7 μm , with steps of 1 μm).

Air trapping on different structures. Here we report additional pictures of air trapping tests on the main sample geometry (Figure S2 and S3) and on other samples with different geometrical parameters. (Figure S4-S6). Notably all the samples that are not able to keep an air layer, are anyhow capable of trapping air inside the crown-like structure.

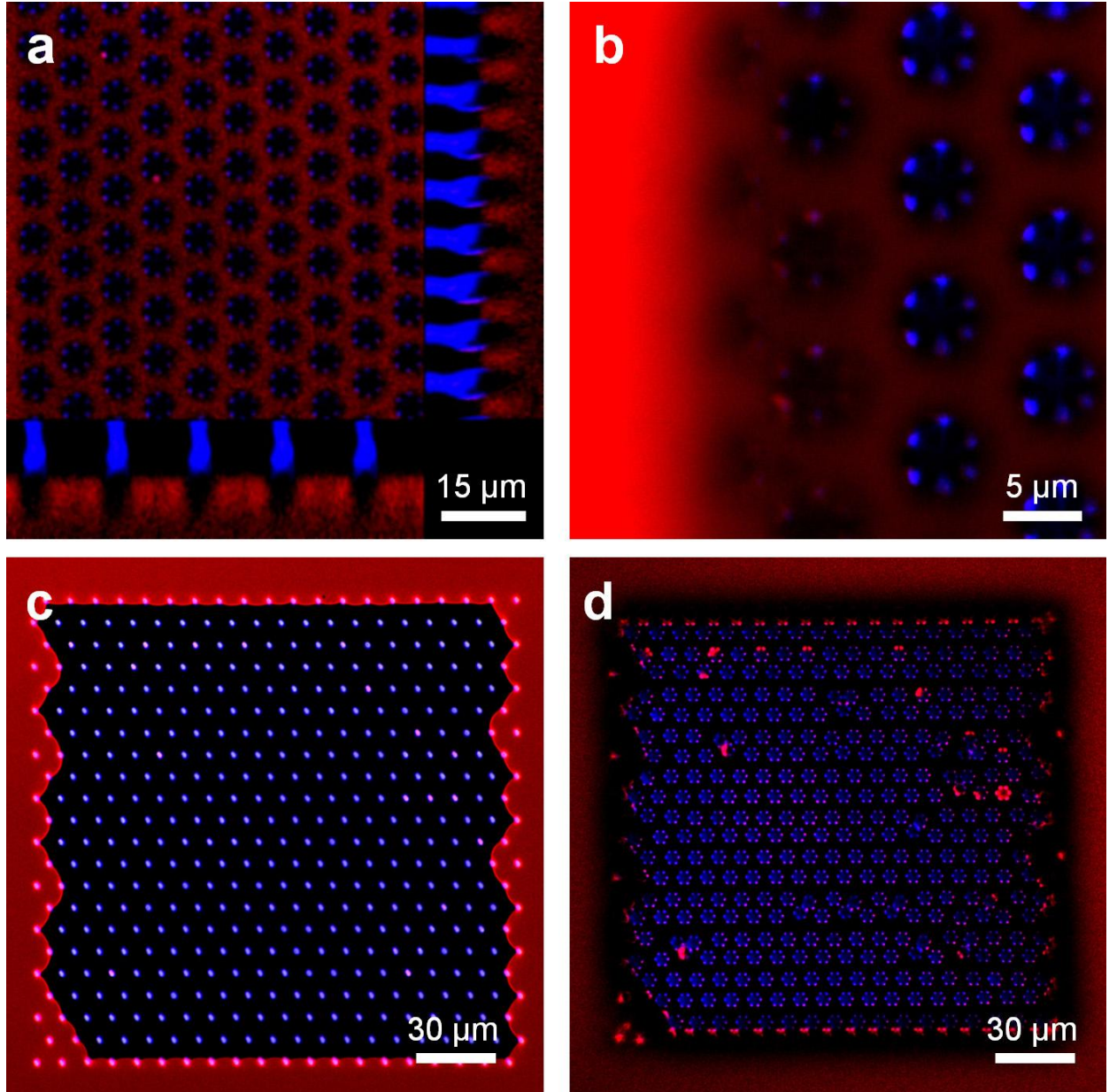


Figure S2. Additional confocal images of the sample presented in main text (square array of hairs with a head-to-head distance of $3\text{ }\mu\text{m}$; hair parameter: $N=3$; $r=3\text{ }\mu\text{m}$; $\delta=1\text{ }\mu\text{m}$; $h=7\text{ }\mu\text{m}$; $w=1.5\text{ }\mu\text{m}$). a) Section at the level of the crown-like heads and the profile of the hairs, showing the presence of air inside the heads. b) Detail of a section of the same micro-patterned surface close to the border of the array. Section of the whole micro-patterned surface at the level of the stalks (c) and at the level of the crown (d) showing the presence of trapped air.

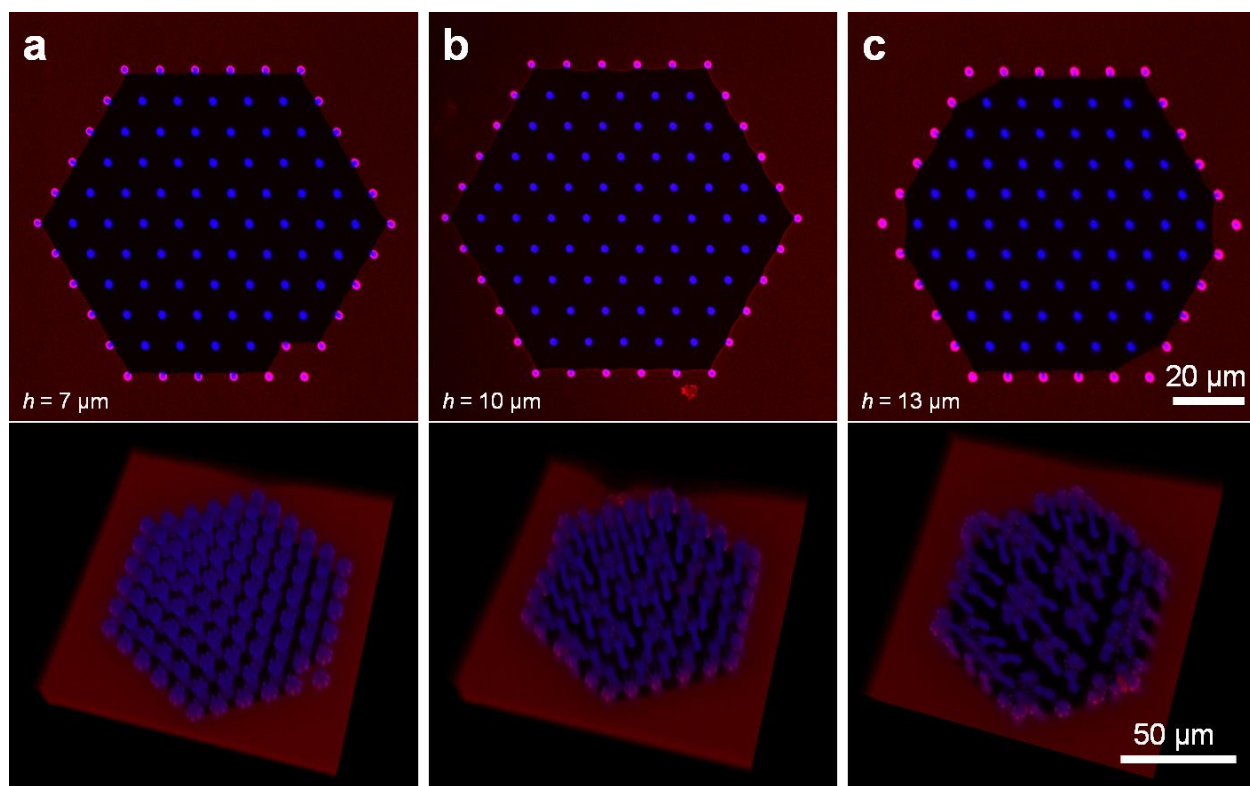


Figure S3. Trapping air test (sections and 3D reconstruction) performed on hexagonal arrays with variable stalk length: $h = 7 \mu\text{m}$ (a), $10 \mu\text{m}$ (b), $13 \mu\text{m}$ (c). (Other hair parameters: $N = 3$; $r = 3 \mu\text{m}$; $\delta = 1 \mu\text{m}$; $w = 1.5 \mu\text{m}$; head-to-head distance of $3 \mu\text{m}$). Noticeably longer and bunched hairs are still able to trap the air inside the structure.

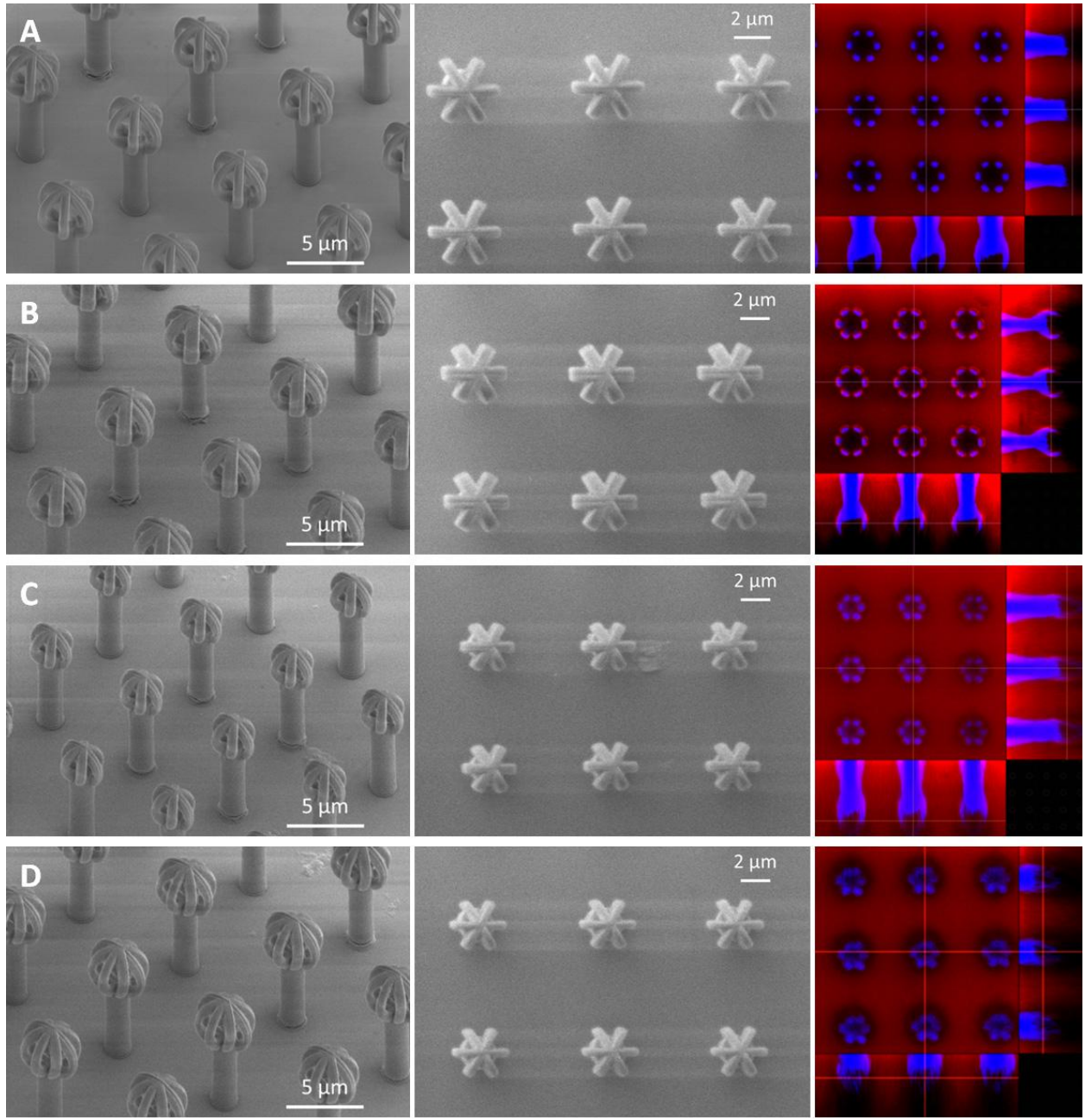


Figure S4. SEM images (left and center) and confocal images (right) of not-air trapping extra samples with following parameters:

Sample A - $N = 3$; $r = 2 \mu\text{m}$; $\delta = 0.65 \mu\text{m}$; $h = 7 \mu\text{m}$; $w = 1.5 \mu\text{m}$ stalk-to-stalk distance: $8 \mu\text{m}$;

Sample B - $N = 3$; $r = 2 \mu\text{m}$; $\delta = 1 \mu\text{m}$; $h = 7 \mu\text{m}$; $w = 1.5 \mu\text{m}$ stalk-to-stalk distance: $8 \mu\text{m}$;

Sample C - $N = 3$; $r = 1.5 \mu\text{m}$; $\delta = 0.63 \mu\text{m}$; $h = 7 \mu\text{m}$; $w = 1.5 \mu\text{m}$ stalk-to-stalk distance: $7 \mu\text{m}$;

Sample D - $N = 3$; $r = 1.5 \mu\text{m}$; $\delta = 0.58 \mu\text{m}$; $h = 7 \mu\text{m}$; $w = 1.5 \mu\text{m}$ stalk-to-stalk distance: $7 \mu\text{m}$.

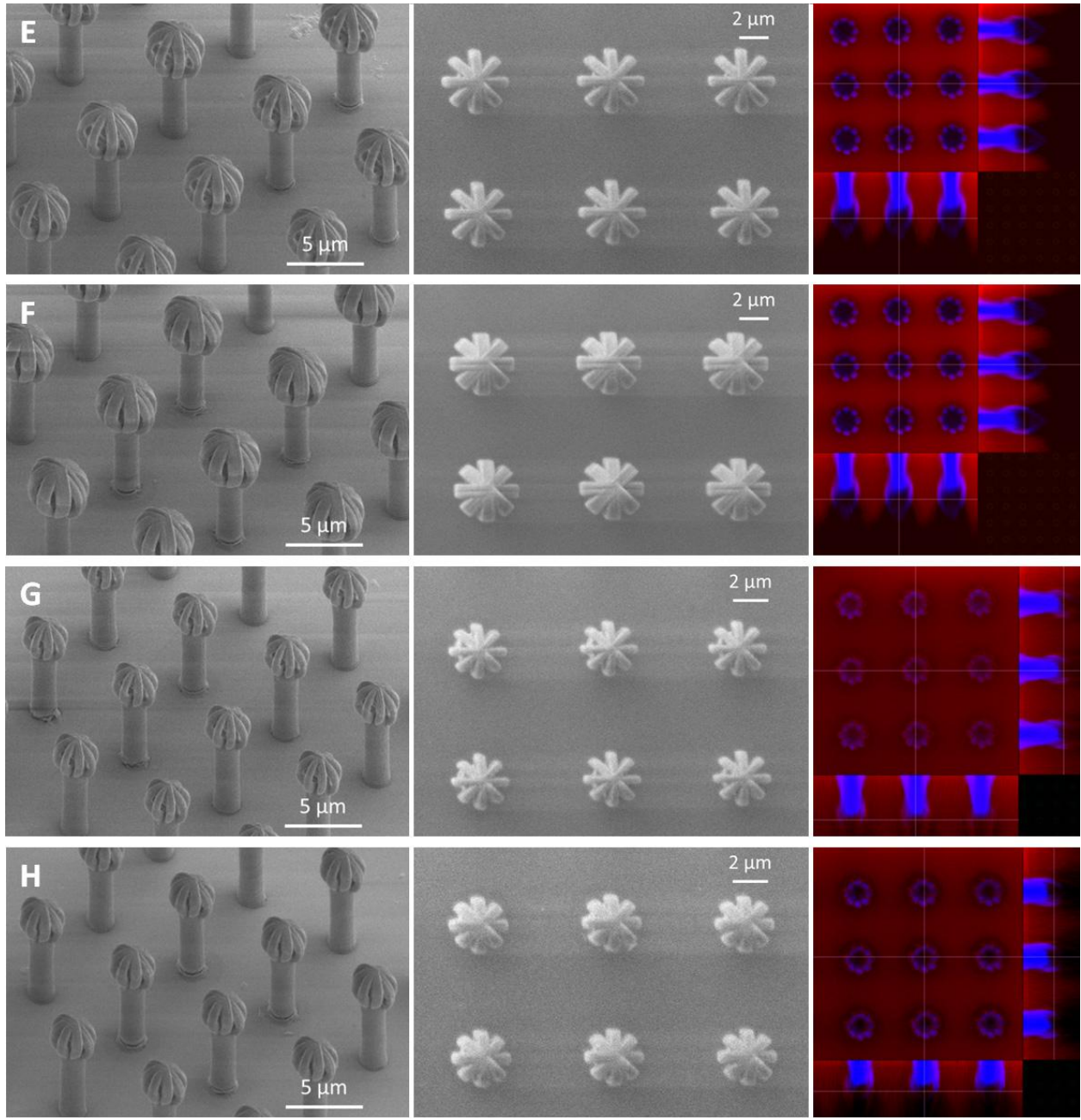


Figure S5. SEM images (left and center) and confocal images (right) of not-air trapping extra samples with following parameters:

Sample E - $N = 4$; $r = 2 \mu\text{m}$; $\delta = 0.66 \mu\text{m}$; $h = 7 \mu\text{m}$; $w = 1.5 \mu\text{m}$ stalk-to-stalk distance: $8 \mu\text{m}$;

Sample F - $N = 4$; $r = 2 \mu\text{m}$; $\delta = 1 \mu\text{m}$; $h = 7 \mu\text{m}$; $w = 1.5 \mu\text{m}$ stalk-to-stalk distance: $8 \mu\text{m}$;

Sample G - $N = 4$; $r = 1.5 \mu\text{m}$; $\delta = 0.49 \mu\text{m}$; $h = 7 \mu\text{m}$; $w = 1.5 \mu\text{m}$ stalk-to-stalk distance: $7 \mu\text{m}$;

Sample H - $N = 4$; $r = 1.5 \mu\text{m}$; $\delta = 0.65 \mu\text{m}$; $h = 7 \mu\text{m}$; $w = 1.5 \mu\text{m}$ stalk-to-stalk distance: $7 \mu\text{m}$.

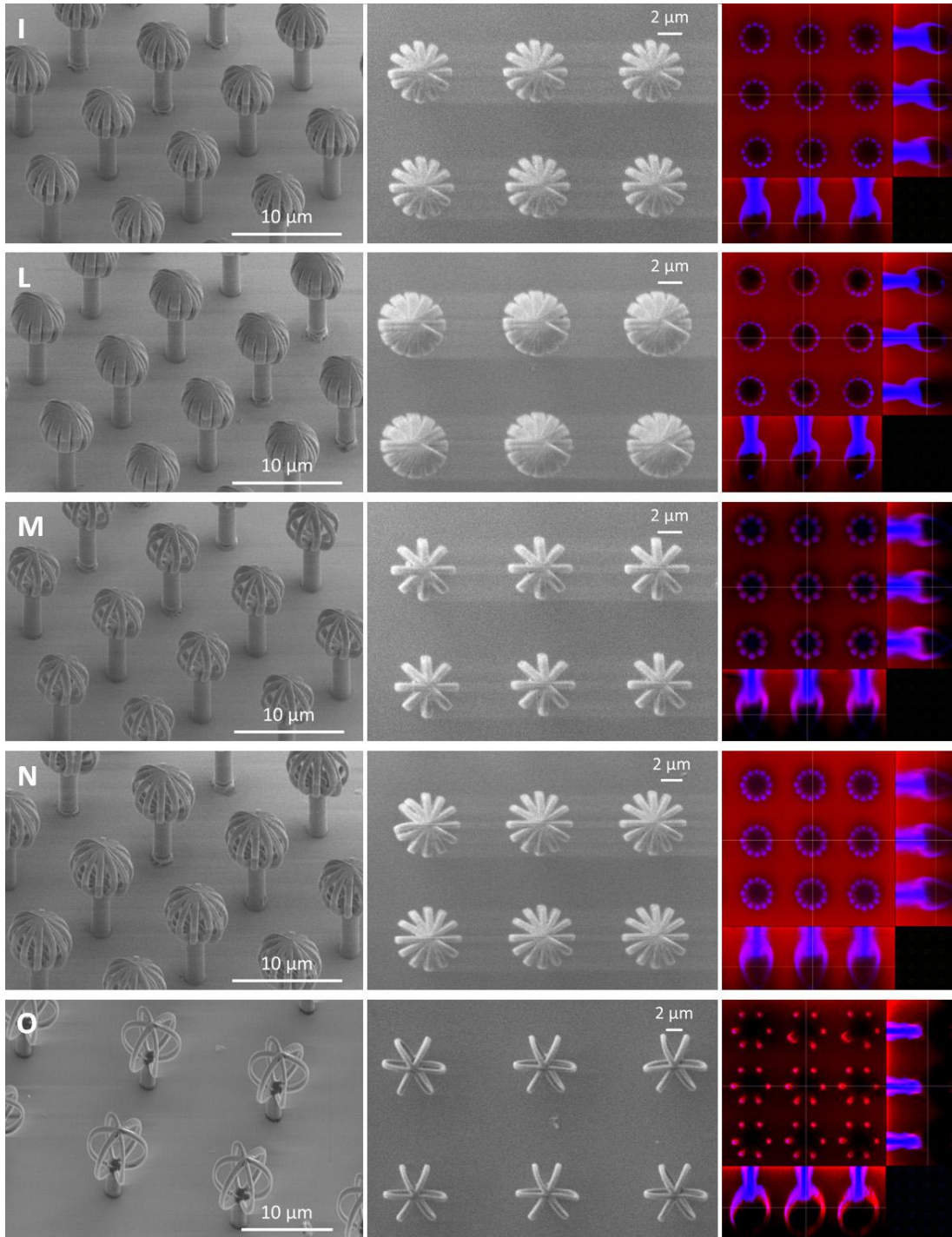


Figure S6. SEM images (left and center) and confocal images (right) of not-air trapping extra samples with following parameters:

Sample I - $N = 6$; $r = 2.5 \mu\text{m}$; $\delta = 0.7 \mu\text{m}$; $h = 7 \mu\text{m}$; $w = 1.5 \mu\text{m}$ stalk-to-stalk distance: $9 \mu\text{m}$;

Sample L - $N = 6$; $r = 2.5 \mu\text{m}$; $\delta = 1 \mu\text{m}$; $h = 7 \mu\text{m}$; $w = 1.5 \mu\text{m}$ stalk-to-stalk distance: $9 \mu\text{m}$;

Sample M - $N = 4$; $r = 2.5 \mu\text{m}$; $\delta = 0.68 \mu\text{m}$; $h = 7 \mu\text{m}$; $w = 1.5 \mu\text{m}$ stalk-to-stalk distance: $9 \mu\text{m}$;

Sample N - $N = 6$; $r = 3 \mu\text{m}$; $\delta = 0.8 \mu\text{m}$; $h = 7 \mu\text{m}$; $w = 1.5 \mu\text{m}$ stalk-to-stalk distance: $10 \mu\text{m}$;

Sample O - $N = 3$; $r = 4 \mu\text{m}$; $\delta = 0.75 \mu\text{m}$; $h = 7 \mu\text{m}$; $w = 1.5 \mu\text{m}$ stalk-to-stalk distance: $11 \mu\text{m}$.

CB-CB CA calculation

CB-CB equation (2) estimates the macroscopic apparent contact angle (θ_{CB}^{CB}) of a liquid on a structured surface when air pockets are trapped in between liquid-solid interface. This is the experimentally observed state. Accordingly, predicted apparent contact angle (θ_{CB}^{CB}) is given by:

$$\theta_{CB}^{CB} = \arccos(F_{SL} \cos(\theta) - 1 + F_{SL}) \quad (S1)$$

where F_{SL} represents the fraction of solid-liquid interface and $\theta = 53^\circ$ is the contact angle of the pristine flat material composing the structured surface.

The interpretation of F_{SL} is not unique here due to the peculiar micro geometry of the crown-head. The simplest assumption is to calculate it as the projection of this structure on a horizontal plane divided by the area of the unitary hexagonal cell, basically assuming an equivalent cylindrical crown-head. This assumption would lead to $F_{SL} = 0.20$ and according to eq. S1 to $\theta_{CB}^{CB} = 133^\circ$. On the other hand, considering the spherical geometry of the crown-head, F_{SL} could be estimated multiplying the previous estimation by the ratio of the real area of the crown-head in contact with water, nearly semispherical, and its projection; in this case we have $F_{SL} = 0.33$, leading to $\theta_{CB}^{CB} = 120^\circ$. Note that the experimental observed CA is of 122° and is thus in between to these “limiting” predictions, but more close to the "semispherical" approximation that considers out-of-the-plane geometry.

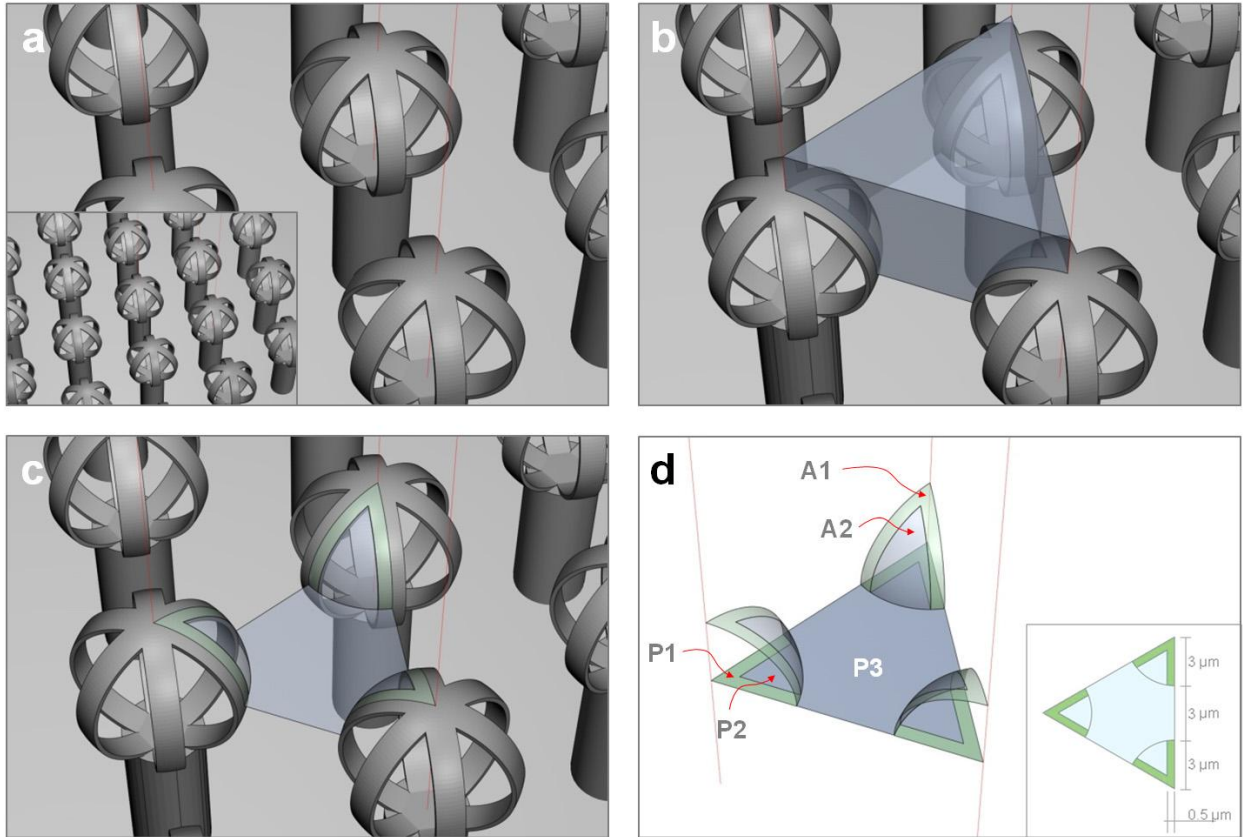


Figure S7. Schematic representation of the micro-structured surface (a) with highlighted the solid-liquid and liquid-air interfaces on a unitary cell (b-c); d) projection of the interfaces on the horizontal plane passing through the centers of crown structures. F_{SL} for equation (S1) is calculated in the first case (flat case) as $F_{SL} = [3 \cdot P1 / (3 \cdot P1 + 3 \cdot P2 + P3)] = 0.20$; in the second case $F_{SL} = [3 \cdot A1 / (3 \cdot P1 + 3 \cdot P2 + P3)] = 0.33$.

Water condensation test. For the final condensation analysis with the environmental scanning electron microscope, the sample (patterned following the previously described experimental procedure), was a square of silicon wafer with a side of 1 cm. It was put on a Peltier cell that provided cooling of sample at $T = 1.0\text{ }^{\circ}\text{C}$ and then placed in the eSEM chamber at a pressure of 640 Pa.

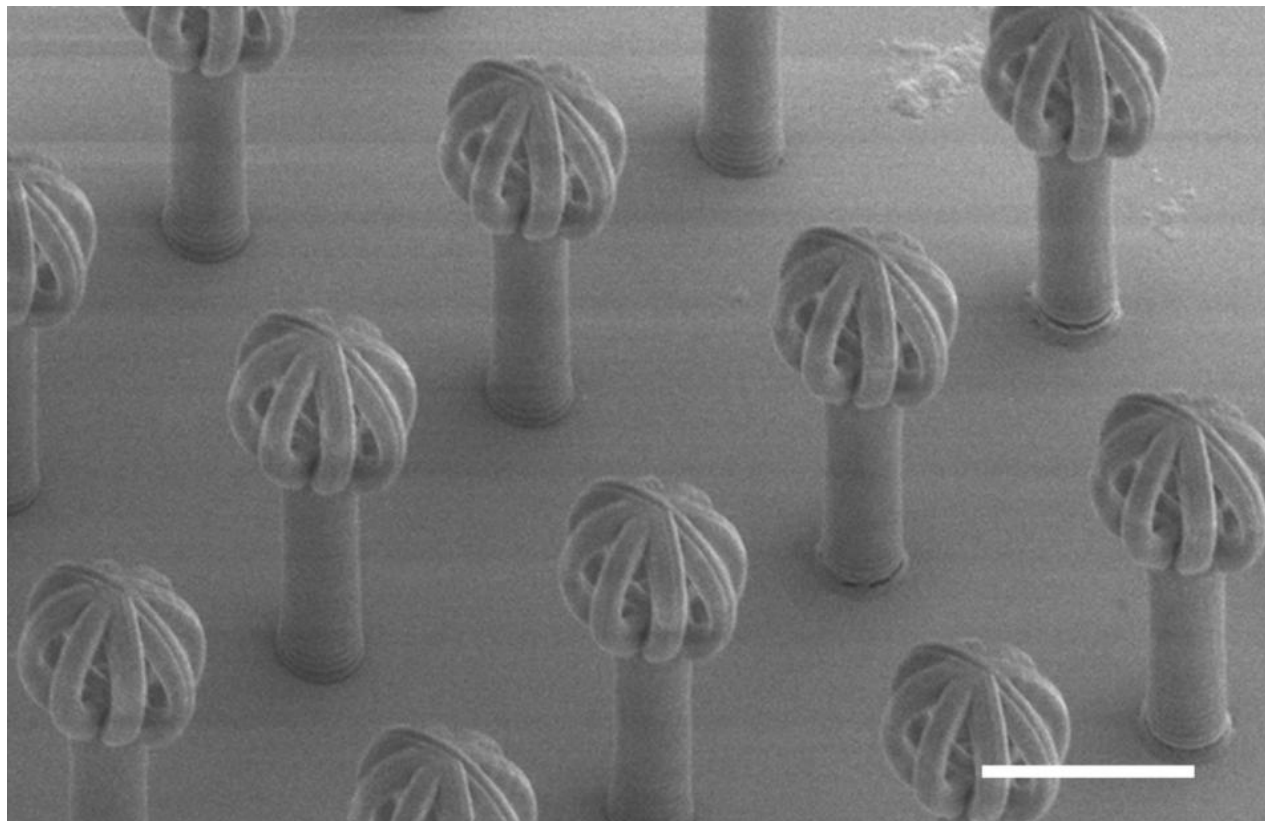


Figure S8. Artificial hairs used in the final condensation test. The diameter of the heads measures $4\text{ }\mu\text{m}$ while the thickness of its filaments is 650 nm . The full sample is composed by a square array of 20×20 elements: the distance between nearest neighbour elements (stalk to stalk) is $5\text{ }\mu\text{m}$.

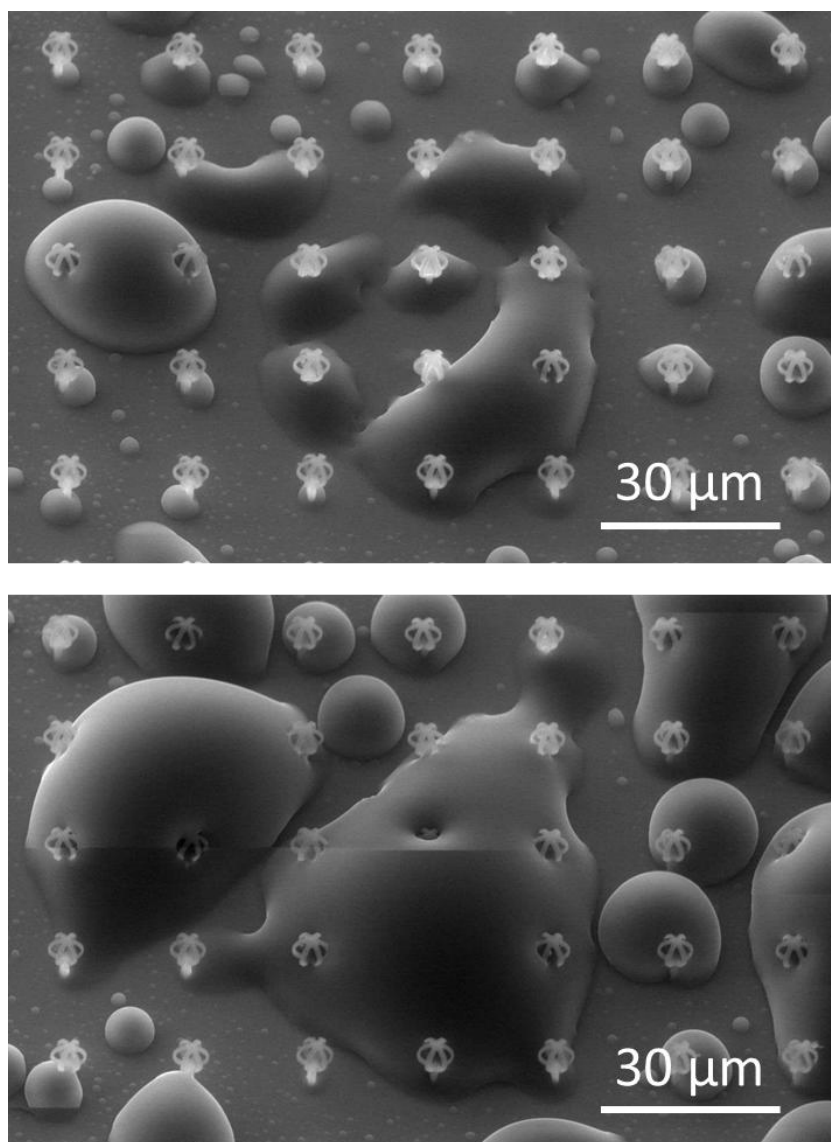


Figure S9. Extra condensation experiment on artificial hairs with head diameter of 6 μm and filaments thickness of 1 μm . The hairs are arranged in a square array with a distance of 20 μm between adjacent stalks. The vapor pressure in the chamber of the eSEM is 815 Pa and the cooling stage temperature is 3.0 $^{\circ}\text{C}$.